

## Right- and left-handed twist in optical fibers

D. Tentori and A. Garcia-Weidner\*

*Centro de Investigación Científica y Educación Superior de Ensenada, Div. Física Aplicada,  
carretera Ensenada-Tijuana No. 3918, Ensenada BC 22860, México.*

\*e-mail: [agarcia@cicese.mx](mailto:agarcia@cicese.mx)

Received 16 August 2013; accepted 17 October 2013

The effect of twist-induced variation of the output state of polarization on clockwise and counterclockwise torsion was measured in two standard optical fibers made by different manufacturers. It was found that standard fiber samples may exhibit a different twist-induced polarization performance for right- and left-handed twists. In this work we compare the results obtained for two commercial fibers using linearly polarized input signals with azimuth angles between 0 and 150°, within the 1520-1570 nm spectral range. In all cases these results could be described using the same theoretical model. We demonstrate that the different behavior observed for right- and left-handed twists for one of the samples can be explained by the presence of a residual torsion.

*Keywords:* Fiber optics; birefringence; polarization.

PACS: 42.81.-i; 42.81.Gs; 42.25.Ja

### 1. Introduction

Twist-induced birefringence in single-mode fibers affects the performances of numerous fiber devices; therefore it has been experimentally studied by several authors and modeled using different approaches. In most of these theoretical descriptions it has been assumed that when an optical fiber is twisted the effect of ellipse rotation progresses monotonically [1-4], making no distinction between clockwise and counterclockwise directions. Based on this idea, it has been concluded that the birefringence induced by equal lengths of the same fiber, twisted in opposite directions cancels out [5], and that the effect of the continuous twist of a specific single mode fiber is the same for right- or left-handed torsions.

Twisting different types of single-mode fibers we found that while some of them exhibit an identical response to right- and left-handed twists (SMF-28 and SMF-28e) [6], for other fibers (erbium-doped [7] and photonic [8]), the response was direction-dependent. To avoid confounding effects, in this work we compare the results obtained for two standard single-mode fibers, Corning SMF-28e and Nufern 1060-XP. We found that for the 1060-XP sample the response to right- and left-handed twist was dissimilar. In this paper, we compare the experimental results obtained for both fibers using monochromatic linearly polarized signals, and make use of the same theoretical model, [6] adding a residual torsion for the 1060-XP fiber, to explain its performance.

### 2. Theory

Due to various imperfections, such as core ellipticity and internal stresses, single-mode optical fibers are birefringent. In general, the magnitude and orientation of this unwanted birefringence are considered to vary randomly along the fiber. However, most fiber devices are built with short fiber lengths (< 50 m), and for such lengths, it can be considered that any non-polarization-maintaining fiber exhibits a uniform residual birefringence.

Under this scope and using a perturbative approach, more than 30 years ago, Ulrich *et al.* [1] proposed that twist-induced birefringence in single-mode fibers induces circular birefringence. If we use  $1 \times 3$  Stokes vectors and  $3 \times 3$  Mueller sub-matrices, circular birefringence can be represented by a rotation matrix  $\mathbf{R}(U)$ ,

$$R(U) = \begin{pmatrix} \cos 2U & -\sin 2U & 0 \\ \sin 2U & \cos 2U & 0 \\ 0 & 0 & 1 \end{pmatrix} \quad (1)$$

$$U = \tau g \quad (2)$$

where  $\tau$  is the applied twist and  $g \approx 0.146$  for silica fibers [1-10]. Ulrich's angle  $U$  was derived considering only the photoelastic contribution to the twist-induced birefringence. As we can see, matrix  $\mathbf{R}(U)$  predicts the same behavior for right- and left-handed twist in optical fibers, making no distinction between clockwise and counterclockwise directions.

Since birefringence is highly sensitive to stresses induced by external fields (electric, magnetic, mechanical, thermal) to validate their experimental results several authors have developed measurement procedures in which one of these perturbations is the test probe [1-4,9-12]. Although it is correct to assume that a finite birefringence induced by a certain external field can dominate over the unintentional birefringence introduced during the fabrication process, it is evident that the results of such an assessment cannot provide information of residual birefringence. We consider that in this work information about the original state of the fiber is required to understand the birefringence results produced by the gradual changes in the applied torsion. Therefore we use the matrix model developed in a previous work, in which the theoretical results for an applied twist that varied from 0 to 1440° using a 5° step were validated measuring the input and output states of polarization with a polarimetric setup [6]. We have shown that for a standard single-mode fiber (SMF-28, SMF-28e) twist-induced birefringence can be described using the matrix model:

$$\mathbf{M}_T(\tau, \delta, \sigma, \beta) = \mathbf{R}(\theta) [\mathbf{R}(\beta + b\tau) \mathbf{M}(\delta, \sigma)] \mathbf{R}(-\theta), \quad (3)$$

$$\mathbf{M}_T(\delta, \sigma) = \begin{pmatrix} 1 - 2 \cos^2 \sigma \sin^2 \frac{\delta}{2} & -\cos \sigma \sin \delta & -\sin 2\sigma \sin^2 \frac{\delta}{2} \\ \cos \sigma \sin \delta & \cos \delta & \sin \sigma \sin \delta \\ -\sin 2\sigma \sin^2 \frac{\delta}{2} & -\sin \sigma \sin \delta & 1 - 2 \sin^2 \sigma \sin^2 \frac{\delta}{2} \end{pmatrix} \quad (4)$$

where  $\mathbf{M}(\delta, \sigma)$  is the Mueller matrix of an elliptical retarder with fixed ellipticity angle  $\varepsilon(\sigma = \pi/2 - 2\varepsilon)$  [13], whose fast birefringence axis has an azimuth angle  $\theta$ ; the retardation angle between the polarization eigenmodes is  $\delta = \delta_0 + c\tau$  (here,  $\delta_0$  is the retardation angle between elliptical eigenmodes when the fiber is not twisted, and  $c$  is a constant);  $\mathbf{R}(\theta)$ ,  $\mathbf{R}(\beta + b\tau)$  and  $\mathbf{R}(-\theta)$  are rotation matrices of the form given by Eq. (1);  $b$  is a constant (the product  $b\tau$  describes the geometrical rotation of the birefringence axes due to torsion [14]);  $\beta$  is a fixed rotation angle and  $\theta$  is the angle between the fiber's eigen axes and the laboratory coordinate system. We can note that the matrix in Eq. (4) does not predict a different behavior for right- and left-handed twists.

The values of parameters  $\theta$ ,  $\sigma$ ,  $\delta_0$ ,  $b$ ,  $c$  and  $\beta$  can be obtained from the numerical fit of the theoretical model predictions to the experimental values measured in the laboratory. The Stokes parameters of the linear input polarization state  $S_{\text{in}} = (\cos 2\varphi, \sin 2\varphi, 0)$  with azimuth angle  $\varphi$ , are related with those of the output polarization state  $S_{\text{out}}$  for each value of the applied twist  $\tau$ , by

$$S_{\text{out}} = \begin{pmatrix} S1 \text{ out} \\ S2 \text{ out} \\ S3 \text{ out} \end{pmatrix} = M_T(\tau, \delta, \sigma, \beta) \begin{pmatrix} \cos 2\varphi \\ \sin 2\varphi \\ 0 \end{pmatrix} \quad (5)$$

and substituting Eq. (3) we obtain,

$$\begin{aligned} S1 \text{ out} &= \cos 2(b\tau + \beta + \theta) \cos 2(\theta - \varphi) \sin^2 \sigma \\ &\quad - \cos \sigma \sin \delta \sin 2(b\tau + \beta + \varphi) \\ &\quad + \cos \delta \{ \cos 2(b\tau + \beta + \theta) \cos^2 \sigma \cos 2(\theta - \varphi) \\ &\quad + \sin 2(b\tau + \beta + \theta) \sin 2(\theta - \varphi) \} \end{aligned} \quad (6)$$

$$\begin{aligned} S2 \text{ out} &= \cos 2(\theta - \varphi) \{ \cos 2(b\tau + \beta + \theta) \cos \sigma \sin \delta \\ &\quad + \sin 2(b\tau + \beta + \varphi) (\cos \delta \cos 2\sigma + \sin^2 \sigma) \} \\ &\quad + \sin 2(\theta - \varphi) \{ \cos \sigma \sin \delta \sin 2(b\tau + \beta + \theta) \\ &\quad - \cos \delta \cos 2(b\tau + \beta + \theta) \}, \end{aligned} \quad (7)$$

$$\begin{aligned} S3 \text{ out} &= \sin \delta \sin \sigma \sin 2(\theta - \varphi) \\ &\quad - \cos 2(\theta - \varphi) \sin^2 \frac{\delta}{2} \sin 2\sigma \end{aligned} \quad (8)$$

### 3. Experiment

To study twist-induced birefringence we used straight and short samples of standard single-mode fibers (SMF-28e, 1.75 m and 1060-XP, 1.5 m). The manufacturer's informa-

tion indicates that tolerances in geometrical and optical specifications are tighter for the 1060-XP fiber, designed to obtain single-mode operation from 980-1600 nm [15]; while for SMF-28e single-mode operation occurs within a narrower range (1285-1575 nm) [16]. There is however no indication of the presence of asymmetries.

Since the specification of a light polarization state demands the definition of a fixed reference frame, an important aspect of the polarization measurement is the use of a set up in which the reference frame is the same at the fiber input and

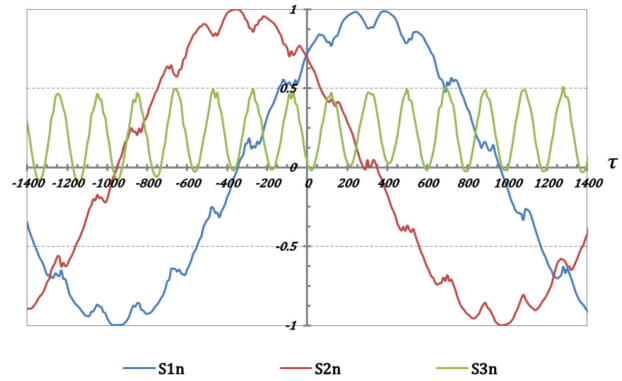


FIGURE 1. Output Stokes parameters  $S1n$ ,  $S2n$  and  $S3n$  measured for a SMF-28e fiber using a linearly polarized input signal (1550 nm, azimuth angle  $\varphi = 30^\circ$ ) and varying the applied torsion  $\tau$  from 0 to  $-1440^\circ$  (right-handed twist) and 0 to  $1440^\circ$  (left-handed twist).

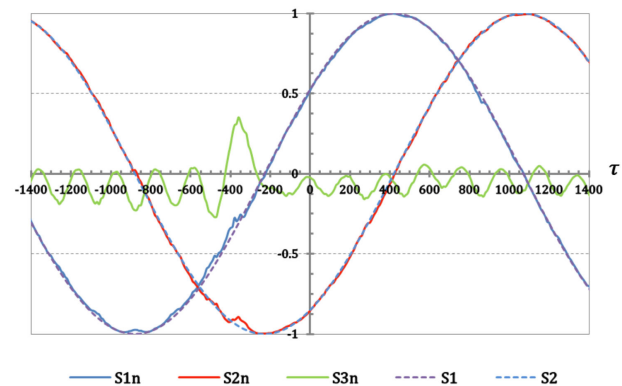


FIGURE 2. Output Stokes parameters  $S1n$ ,  $S2n$  and  $S3n$  measured for a 1060-XP fiber using a linearly polarized input signal (1550 nm, azimuth angle  $\varphi = 30^\circ$ ) and varying the applied torsion  $\tau$  from 0 to  $-1440^\circ$  (right-handed twist) and 0 to  $1440^\circ$  (left-handed twist).

TABLE I. Fitting parameters values used for the 1060-XP fiber (Fig. 4)

Wavelength in nm	Twist direction	$\theta$	$\delta_0$	$c$	$\sigma$	$b$	$\beta$	$\tau_0$
1530	right	$-10^\circ$	$-52^\circ$	-0.9	$6^\circ$	-0.97	$90^\circ$	$-510^\circ$
1530	left	$-20^\circ$	$55^\circ$	0.9	$5^\circ$	0.97	$90^\circ$	$-510^\circ$

output. To fulfill this requirement output Stokes parameters were measured using the polarimetric set-up described in Ref. [6]. We used a linearly polarized input signal, because it is an easily controllable polarization state that offers an additional degree of freedom to elucidate the birefringence response of fibers and fiber devices.

The state of polarization (SOP) and wavelength  $\lambda$  of the input signal remained fixed while the twist angle was varied using  $10^\circ$  steps, from 0 to  $\pm 1440^\circ$  ( $5^\circ$  step). Keeping the same wavelength, the azimuth angle  $\varphi$  was varied  $30^\circ$  to obtain a new set of output Stokes parameters, this procedure was repeated for azimuth angles  $\varphi$  from 0 to  $150^\circ$ . The signal wavelengths applied varied from 1520 to 1570 nm using a 5 nm step. The experimentally obtained Stokes vectors are represented by  $\mathbf{S}_n=(S_{1n},S_{2n},S_{3n})$ . Typical results for each type of fiber are shown in Figs. 1 and 2.

The experimental results measured for Stokes parameters  $S_{1n}$ ,  $S_{2n}$  and  $S_{3n}$  shown in Fig. 1 tell us that for this fiber (SMF-28e) changes induced by torsion follow the same behavior for right- and left-handed twists. Stokes parameters  $S_{1n}$  and  $S_{2n}$  measured for the XP-1060 ( $\lambda = 1555$  nm, azimuth angle  $150^\circ$ ) fiber were fitted in Fig. 2 using cosine and sine functions with the same argument (dotted lines). We can see that for these Stokes parameters the torsion-induced change follows the same behavior for right- and left-handed twists. But, for Stokes component  $S_{3n}$  it is evident that we cannot use the same sine function to describe right- and left-handed twists, since the amplitude and frequency of these oscillations are not equal.

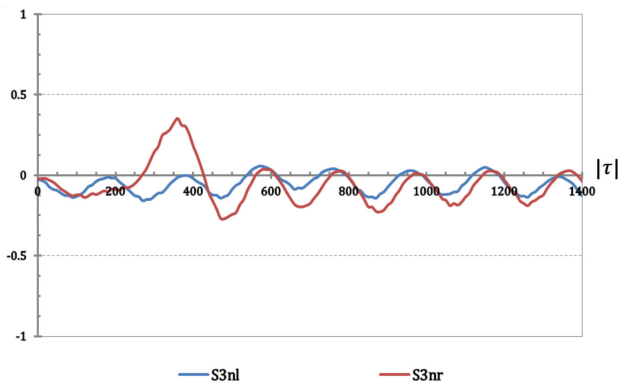


FIGURE 3. Output Stokes parameter  $S_3$  measured for a 1060-XP fiber using a linearly polarized input signal (1555 nm, azimuth angle  $\varphi = 150^\circ$ ) and varying the applied torsion  $|\tau|$  from 0 to  $1440^\circ$ . The blue line corresponds to left-handed ( $S_{3nl}$ ) and the red line to right-handed twist ( $S_{3nr}$ ).

To give emphasis to these changes, in Fig. 3 we present the results measured for Stokes parameter  $S_{3n}$  ( $\lambda=1555$  nm, azimuth angle  $150^\circ$ ) using the absolute value of the torsion angle. We can see that while the values of  $S_{3nr}$  and  $S_{3nl}$  (right-handed and left-handed twists) measured for small twist angles ( $|\tau| < 510^\circ$ ) are very different, it is clear that as the torsion increases ( $|\tau| > 1000^\circ$ ),  $S_{3nr}$  and  $S_{3nl}$  tend to show a similar behavior. This result agrees with the idea that for large torsion angles, twist-induced birefringence becomes dominant.

In the present study we found that we could predict very accurately the Stokes parameters values for right- and left-handed twists with absolute values larger than  $\sim 600^\circ$ , as we can see in Fig. 4 for  $\lambda = 1530$  nm. Here we assumed that the fiber shows a residual twist  $\tau_0$  in such a way that instead of using  $\delta = \delta_0 + c\tau$  we added a new parameter and used

$$\delta = \delta_0 + c(\tau_0 + \tau) \tag{9}$$

with  $\tau_0 = -510^\circ$ . Using Eq. (9) in Eqs. (6) to (8), we obtained the additional six parameter's values  $c$ ,  $b$ ,  $\beta$ ,  $\theta$ ,  $\delta_0$ , and  $\sigma$  shown in Table I.

For the XP-1060 fiber sample in this study, as well as for the samples in the previous work [6],  $\beta = 90^\circ$ . For the XP-1060 fiber the sign of the geometric parameters  $c$  and  $b$  was positive for right-handed torsions and negative for the left-handed twists, keeping a fixed value ( $c = \pm 0.9$ ,  $b = \pm 0.97$ ). Wavelength dependent parameters  $\theta$ ,  $\delta_0$  and  $\sigma$  (Table I) showed a twist direction variation: 1) the azimuth angle of the fast birefringence axis was  $\theta = -10^\circ$  for right-handed torsions and varied to  $\theta = -20^\circ$  for left-handed twists; 2) the retardation angle between polarization eigenmodes with no applied twist ( $\delta_0$ ) was equal to  $-52^\circ$  for a right-handed twist and varied to  $55^\circ$  for a left-handed torsion; 3) the parameter related with the ellipticity angle of the fiber anisotropy ( $\sigma$ ) had also different values for right- and left-handed twists. For a right-handed torsion it was equal to  $6^\circ$  and for a left-handed twist was  $5^\circ$ .

### 4. Discussion

In single-mode fibers total induced birefringence has several origins: geometrical imperfections as well as stress-induced anisotropies produced during the manufacturing process (residual birefringence), and geometrical and stress-induced anisotropy due to the applied torsion [6]. Considering that all of them are acting uniformly along the fiber and

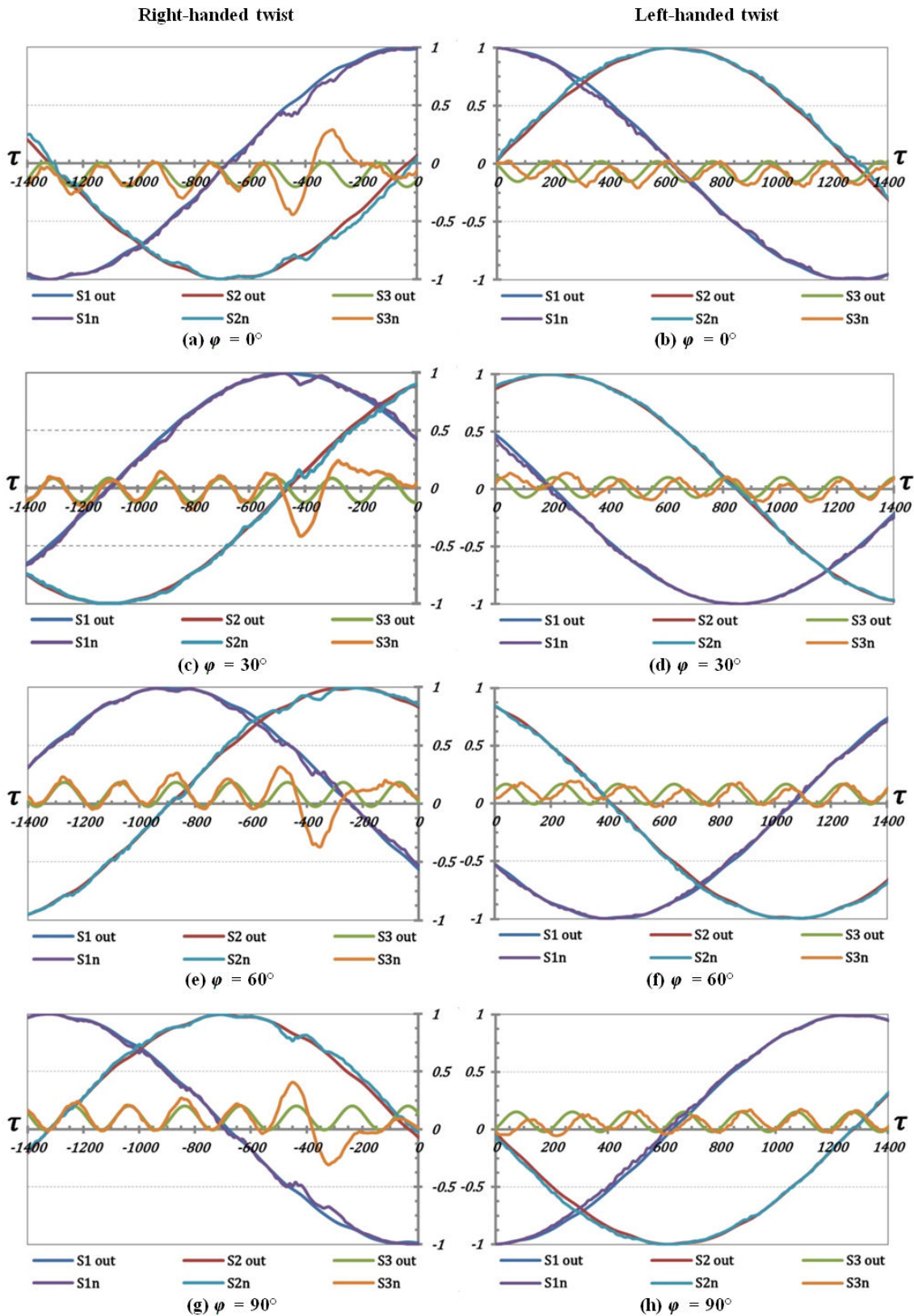


FIGURE 4. Theoretical fitting to the experimental results measured for a linearly polarized 1530 nm signal, for the 1060-XP fiber. The twist applied to the fiber is the horizontal axis. Vertical axis represents the experimental and theoretical values of the Stokes parameters [(S1n, S2n, S3n) and (S1out, S2out, S3out), respectively]. The number below each graph indicates the value of the azimuth angle  $\varphi$  of the input linear polarization.

using the model presented above, we have described in a previous work the experimental results obtained for two types of standard single-mode fibers (SMF-28 and SMF-28e) [6]. For those fibers the geometrical parameters ( $c$ ,  $b$ ,  $\beta$ ) were the same for all the signal wavelengths (1520-1570 nm with a 5 nm step), and wavelength dependent parameters ( $\theta$ ,  $\delta_0$ ,  $\sigma$ ) were the same for all the input azimuth angles used for each signal wavelength (0-150° with a 30° step). As mentioned below, in the present study we found a similar distinction between geometrical and wavelength dependent parameters.

From Fig. 4, it is clear that the results obtained for the Stokes parameter S3 while the applied torsion varied between 0 and -600° are different. We consider that due to the residual right-handed torsion (-510°), for a small left-handed twist (< 510°) the waveguide goes through straightening modifications manifested as uneven variations on parameter S3n (Figs. 2, 3 and 4). Straightening modifications cause additional stress expressed as refractive index changes and wavelength dependent parameters ( $\theta$ ,  $\delta_0$ ,  $\sigma$ ) dissimilarities. Therefore we can link the wavelength sensitivity of parameters  $\theta$ ,  $\delta_0$  and  $\sigma$  to stress-induced refractive index changes. Furthermore, since the assumption of the presence of a residual torsion  $\tau_0$  can explain the different behavior observed for right- and left-handed torsions, and it also helps to fit the experimental data to the theoretical model, we propose that this direction sensitivity is a result of stress and waveguide variations introduced while the residual torsion is reduced. As a result, light propagates as if the fiber with a right-handed twist had a different azimuth angle of the fast birefringence axis ( $\theta$ ) and a different ellipticity angle (associated to parameter  $\sigma$ ) with respect to the same fiber with a left-handed torsion. Nevertheless, the light's SOP progresses along the fiber following a continuous evolution (Fig. 4) that can be described for twists (absolute value) larger than  $\sim 1000^\circ$  using the same theoretical model and similar values for each parameter (Table I).

It is important to remark that our data show that depending on the optical fiber, for small twists, the induced bire-

fringence can be strongly direction-dependent. This new information is relevant for helical coils used in electric current fiber sensors and fiber optic gyroscopes, since in out-of-plane curves torsion is a geometrical consequence.

Comparing the results obtained for SMF-28 and SMF-28e fibers [6], with those measured for XP-1060 we can note that for the last fiber: 1) twist variation of Stokes parameters S1 and S2 was smoother, 2) there was a stronger sensitivity to optical alignment, 3) Stokes parameter S3 presents a lower amplitude variation, 4) Stokes parameter S3 exhibited a different behavior for right- and left-handed torsion. We hypothesize that results 1) to 3) are related to the tighter fabrication tolerances used for the XP-1060 optical fiber and its smaller mode-field diameter [15,16].

The similar response measured for Corning fibers [6] and different polarization performance obtained for the Nufern sample made us think that, as it has been earlier proposed [4], birefringence measurements may provide an effective tool for inspection and testing of fiber production processes, from the drawing to the packing.

## 5. Conclusions

In this work we used a standard single-mode fiber that presented a different behavior for right- and left-handed twists. We have shown that this performance can be explained by the model previously developed [6] by adding a residual torsion.

For some fibers this direction-dependent effect can be significant at the level of small twists, such as those present in helical coils (electric current sensors and fiber optic gyroscopes).

## Acknowledgements

We would like to thank Miguel Farfán Sánchez for his help with data collection.

1. R. Ulrich and A. Simon, *Appl. Opt.* **18** (1979) 2241-2251.
2. A. M. Smith, *Appl. Opt.* **19** (1980) 2606-2611.
3. R. E. Schuh, E. S. R. Sikora, N. G. Walker, A. S. Siddiqui, L. M. Gleeson, and D. H. O. Bebbington, *Electron. Lett.* **31** (1995) 1772-1773.
4. A. Galtarossa and L. Palmieri, *J. Lightwave Technol.* **20** (2002) 1149-1159.
5. N. Mancier, A. Chakari, P. Meyrueis, and P. Clement, *Appl. Opt.* **34** (1995) 6489-6495.
6. D. Tentori, A. García-Weidner and C. Ayala-Díaz, *Opt. Fiber Technol.* **18** (2012) 14-20.
7. D. Tentori, "Twist-induced birefringence in Erbium-doped fibers" in Proceedings of SPIE 7839 2nd Workshop on Specialty Optical Fibers and Their Applications, Oaxaca, (2010), p. 78391.
8. D. Tentori, A. Garcia-Weidner, I. Torres-Gómez, "Twist-induced birefringence in hexagonal photonic fibers" in Proceedings of SPIE 8011 22nd Congress of the International Commission for Optics: Light for the Development of the World, Puebla, (2011) p. 80114.
9. A. Bertholds and R. Dändliker, *J. Lightwave Technol.* **6** (1988) 17-20.
10. M. Monerie and P. Lamouler, *Electron. Lett.* **17** (1981) 252-253.
11. P. Graindorge, K. Thyagarajan, H. Arditty, and M. Papuchon, *Opt. Commun.* **41** (1982) 164-168.

12. T. Chartier, C. Greverie, L. Selle, L. Carlus, G. Bouquet, and L. Montmorillon, *Opt. Express* **11** (2003) 2561-2566.
13. C. Tsao, *Optical Fibre Waveguide Analysis* (Oxford University Press, New York, 1992).
14. D. Tentori, C. Ayala-Díaz, E. Ledezma-Sillas, F. Treviño-Martínez, and A. García-Weidner, *Opt. Commun.* **282** (2009) 830-834.
15. Nufern, “1060-XP, 980/1060 nm Select Cutoff Single-Mode Fiber”, [http://www.nufern.com/pam/optical\\_fibers/424/1060-XP](http://www.nufern.com/pam/optical_fibers/424/1060-XP)
16. Corning, “Corning SMF-28e Optical Fiber Product Information”, [http://www.tlc.unipr.it/cucinotta/cfa/datasheet\\_SMF28e.pdf](http://www.tlc.unipr.it/cucinotta/cfa/datasheet_SMF28e.pdf).